

Hydrothermal Syntheses, Structures, and Fluorescence Spectroscopy of New One-Dimensional Uranium Oxyfluorides Built from Edge-Sharing [UO₂F₅] Pentagonal Bipyramids

Philip M. Almond, Catherine E. Talley, Amanda C. Bean, Shane M. Peper, and Thomas E. Albrecht-Schmitt¹

Department of Chemistry, Auburn University, Auburn, Alabama 36849

Received June 6, 2000; in revised form July 12, 2000; accepted July 28, 2000; published online September 30, 2000

Three new one-dimensional uranium oxyfluorides, (C₅H₁₄N₂)U₂O₄F₆ (AU1-3), (C₅H₆N)UO₂F₃ (AU1-4), and (C₃H₅N₂)UO₂F₃ (AU1-5), have been prepared from the reactions of UO₃ with HF and homopiperazine (C₅H₁₂N₂), pyridine, or pyrazole at 180°C in aqueous media. In all cases, the compounds were isolated in high yield in the form of large single crystals. Single crystal X-ray diffraction, elemental analysis, and fluorescence spectroscopy have been used to characterize these compounds. Each structure contains linear one-dimensional chains formed from edge-sharing [UO₂F₅] pentagonal bipyramids with substantial hydrogen-bonding occurring between the protonated organic cations and the anionic chains. AU1-4 and AU1-5 luminesce brightly when irradiated with 365 nm UV light, while emission is considerably weaker from AU1-3. An energy transfer mechanism between the pyridinium and pyrazolium cations and the UO₂²⁺ groups in AU1-4 and AU1-5, respectively, is proposed to account for some of these differences. Crystallographic data: AU1-3, triclinic, space group *P* $\bar{1}$, *a* = 7.328(2) Å, *b* = 9.488(3) Å, *c* = 11.106(4) Å, α = 94.65(3)°, β = 106.47(3)°, γ = 107.79(2)°, *Z* = 2, MoK α , λ = 0.71073, *R*(*F*) = 5.02% for 173 parameters with 1977 reflections with *I* > 2 σ (*I*); AU1-4, orthorhombic, space group *Imma*, *a* = 6.793(2) Å, *b* = 7.232(2) Å, *c* = 17.094(7) Å, *Z* = 4, MoK α , λ = 0.71073, *R*(*F*) = 3.14% for 44 parameters with 412 reflections with *I* > 2 σ (*I*); AU1-5, monoclinic *C*2/*m*, *a* = 17.011(7) Å, *b* = 6.708(3) Å, *c* = 7.213(2) Å, β = 113.31(3)°, *Z* = 4, MoK α , λ = 0.71073, *R*(*F*) = 3.76% for 65 parameters with 664 reflections with *I* > 2 σ (*I*). © 2000 Academic Press

INTRODUCTION

Investigations of hydrothermal reactions of transition metal oxides with a variety of mineralizing agents, especially fluoride, phosphate, and hydroxide, have resulted in the discovery of numerous low-dimensional and open-frame-

work materials that display significant physiochemical properties such as molecular sieving, catalysis, and magnetic transitions (1–17). These explorations have been broadened to include organically templated reactions of uranium compounds with fluoride (18–23), molybdate (24), and phosphate (25), allowing for the isolation of a diverse series of uranium(IV) fluorides and uranium(VI) oxyfluorides, molybdates, and phosphates. These compounds typically form low-dimensional inorganic architectures as observed in (C₅H₁₄N₂)₂U₂F₁₂·2H₂O (23), which contains [U₂F₁₂]⁴⁻ one-dimensional chains, and (H₃N(CH₂)_nNH₃)U₂F₁₀ (*n* = 2 (23), 3 (18, 19), 5 (18, 19), 6 (18, 19)) all of which possess [U₂F₁₀]²⁻ two-dimensional sheets. These compounds possess a rich variety of properties including ion-exchange (18, 19) and magnetic transitions (18, 19, 23). For instance, the diprotonated diaminoalkanes in the aforementioned layered compounds can be easily exchanged with alkali metal cations and Co(II), providing a low-temperature route to new ternary phases (19). Low-dimensional U(VI) phosphonates (26–29) have also been prepared, and these, too, exhibit unusual characteristics such as room temperature phase transformations (30). Furthermore, those materials containing U(IV) display a number of magnetic properties including antiferromagnetic (18, 19, 23) and ferromagnetic (23) behavior, as well as metamagnetic transitions (23).

Compounds containing isolated [UO₂F₅]³⁻ pentagonal bipyramids are well established in the solid state, being built around the highly stable uranyl, UO₂²⁺, cation (31). [UO₂F₅]³⁻ anions can consolidate through edge and corner sharing to form dimers, as in K₅(UO₂)₂F₉ (32), and can further condense into one-dimensional chains as observed in K₃(UO₂)₂F₇·2H₂O (33). O'Hare and coworkers have reported two-dimensional sheets formed from these polyhedra in (C₄H₁₂N₂)₂(U₂O₄F₅)₄·11H₂O (22). Finally, this connectivity can be extended into three dimensions to yield open-framework compounds, as found for (C₄H₁₂N₂)U₂

¹ To whom correspondence should be addressed. Fax: (334) 844-6959. E-mail: albreth@auburn.edu.



O₄F₆ (21). Herein we report the hydrothermal syntheses, structures, and fluorescence spectra of three new uranium oxyfluorides, (C₅H₁₄N₂)U₂O₄F₆ (**AU1-3**), (C₅H₆N)UO₂F₃ (**AU1-4**), and (C₃H₅N₂)UO₂F₃ (**AU1-5**), all of which contain linear, one-dimensional chains formed from edge-sharing [UO₂F₅] polyhedra. We also provide evidence that accounts for the redox processes taking place in the hydrothermal syntheses of organically templated actinides.

EXPERIMENTAL

Syntheses. UO₃ (99.8%, Alfa-Aesar), HF (48 wt%, Aldrich), homopiperazine (98%, Aldrich), pyrazole (98%), and HF·pyridine (70 wt% HF) were used as received. Distilled and millipore filtered water was used in all reactions. The resistance of the water was 18.2 MΩ. *While the UO₃ contains depleted U, standard precautions for handling radioactive materials should be followed.* Elemental (CHN) microanalyses were performed by Atlantic Microlab, Inc. All reactions were run in Parr 4749 23-mL autoclaves with PTFE liners. The naming system for these compounds stands for Auburn University, the dimensionality of the structure, and the compound number.

(C₅H₁₄N₂)U₂O₄F₆ (**AU1-3**). UO₃ (1.144 g, 4 mmol) and homopiperazine (200 mg, 2 mmol) were loaded in a 23-mL PTFE-lined autoclave. Water (1 mL) was then added to the solids, followed by dropwise addition of HF (0.51 mL, 14.1 mmol). The autoclave was sealed and placed in a box furnace that had been preheated to 180°C. After 72 h the furnace was cooled at 9°C/h to 23°C. The product consisted of a light brown solution over yellow needles and yellow truncated rectangular bipyramids. Crystals of both habits were established to be the same compound by single crystal X-ray diffraction. The mother liquor was decanted from the crystals, which were then washed with methanol and allowed to dry; yield, 1.240 g (82% yield). Anal. Calcd. for C₅H₁₄N₂F₆O₄U₂: C, 7.94; H, 1.87; N, 3.70. Found: C, 7.81; H, 1.84; N, 3.63.

(C₅H₆N)UO₂F₃ (**AU1-4**). UO₃ (286 mg, 1 mmol) was loaded in a 23-mL PTFE-lined autoclave, followed by the addition of 1 mL of water. HF·pyridine (1.09 mL, approximately 38 mmol HF, and 4.1 mmol pyridine) was then added dropwise to the reaction mixture. The autoclave was sealed and placed in a box furnace that had been preheated to 180°C. After 72 h the furnace was cooled at 9°C/h to 23°C. The product consisted of a faintly yellow solution over large bright yellow crystals with an approximately truncated rectangular bipyramidal habit. The mother liquor was decanted from the crystals, which were then washed with methanol and allowed to dry; yield, 315 mg (77% yield). Anal. Calcd. for C₅H₆NF₃O₂U: C, 14.75; H, 1.49; N, 3.44. Found: C, 14.25; H, 1.46; N, 3.32.

(C₃H₅N₂)UO₂F₃ (**AU1-5**). UO₃ (572 mg, 2 mmol) and pyrazole (156 mg, 2.3 mmol) were loaded in a 23-mL PTFE-lined autoclave. Water (1 mL) was then added to the solids, followed by drop-wise addition of HF (0.75 mL, 20.7 mmol). The autoclave was sealed and placed in a box furnace that had been preheated to 180°C. After 72 h the furnace was cooled at 9°C/h to 23°C. The product consisted of an almost clear yellow solution over pale yellow crystals that had a truncated rectangular bipyramidal habit. The mother liquor was decanted from the crystals, which were then washed with methanol and allowed to dry; yield, 644 mg (81% yield). Anal. Calcd. for C₃H₅N₂F₃O₂U: C, 9.10; H, 1.27; N, 7.07. Found: C, 9.23; H, 1.28; N, 7.09.

Crystallographic studies. Intensity data were collected from single crystals of **AU1-3**, **AU1-4**, and **AU1-5** with the use of a Nicolet R3M X-ray diffractometer. Data for each compound were processed and analytical absorption corrections were applied. The structures were solved by direct methods and refined using the SHELXTL-93 package (34). The structure solutions for all compounds were relatively straightforward with three exceptions. First, the nitrogen atoms in rings of pyrazole and pyridine were placed at sites where optimal hydrogen bonding was present. However, disorder with carbon atoms over several sites is suspected, though not resolvable. Second, in **AU1-4**, the pyridine ring is rotationally disordered, with six carbon sites being resolved. The occupancy of the appropriate carbon site was set to 0.50. Third, the anisotropic thermal parameters for **AU1-4** show slight elongation and have forced the collection of data sets from multiple crystals to ensure proper corrections for absorption and extinction. In all cases roughly the same elongation is observed which may indicate intimate twinning or perhaps stacking disorder (35). The only data that possibly indicate this are the elongated ellipsoids, which refine anisotropically without going nonpositive definite. Furthermore, peak scans demonstrate very sharp diffraction peaks without observable shoulders. Some crystallographic details are listed in Table 1 for **AU1-3**, **AU1-4**, and **AU1-5**. The final positional parameters for **AU1-3**, **AU1-4**, and **AU1-5** are given in Tables 2–4.

Fluorescence spectroscopy. Crystals used for spectral measurements were placed onto a microscope slide, rinsed with a drop of methanol, and covered with a glass coverslip. Emission spectra of single crystals were collected using a Nikon Eclipse E400 microscope equipped with an epifluorescence attachment (Southern Micro Instruments), and an imaging spectrometer (Lightform Inc.) coupled to a CCD detector (Electrim Corp.). Light from a 100-W Hg arc lamp was passed through an excitation filter (425–475 nm), reflected by a dichroic mirror (480 nm), and focused onto a crystal by 40× (0.75 NA) objective lens. The fluorescence emitted was collected by the objective lens, transmitted through the dichroic mirror, and passed through a long-pass emission

TABLE 1
Crystallographic Data for (C₅H₁₄N₂)U₂O₄F₆ (AU1-3), (C₅H₆N)UO₂F₃ (AU1-4), and (C₃H₅N₂)UO₂F₃ (AU1-5)

Formula	(C ₅ H ₁₄ N ₂)U ₂ O ₄ F ₆	(C ₅ H ₆ N)UO ₂ F ₃	(C ₃ H ₅ N ₂)UO ₂ F ₃
Formula mass (amu)	756.24	407.14	396.12
Color and habit	Yellow, needle	Yellow, truncated rectangular	Yellow, truncated rectangular
Space group	<i>P</i> $\bar{1}$ (No. 2)	<i>Imma</i> (No. 74)	<i>C2/m</i> (No. 12)
<i>a</i> (Å)	7.328(2)	6.793(2)	17.011(7)
<i>b</i> (Å)	9.488(3)	7.232(2)	6.708(3)
<i>c</i> (Å)	11.106(4)	17.094(7)	7.213(2)
α (deg.)	94.65(3)	90	90
β (deg.)	106.47(3)	90	113.31(3)
γ (deg.)	107.79(2)	90	90
<i>V</i> (Å ³)	693.1(4)	839.8(5)	755.9(5)
<i>Z</i>	2	4	4
<i>T</i> (°C)	22	22	22
λ (Å)	0.710 73	0.710 73	0.710 73
Maximum 2θ (deg.)	50	50	50
Observed data	1977 (0.0339)	412 (0.0200)	664 (0.0203)
<i>I</i> > 2 σ (<i>I</i>)			
ρ_{calcd} (g cm ⁻³)	3.624	3.220	3.481
μ (MoK α) (cm ⁻¹)	234.15	193.39	214.83
<i>R</i> (<i>F</i>) for	0.0502	0.0312	0.0376
$F_o^2 > 2\sigma(F_o^2)^a$			
$R_w(F_o^2)^b$	0.1338	0.0817	0.1128

$$^a R(F) = \frac{\sum ||F_o| - |F_c||}{\sum |F_o|}$$

$$^b R_w(F_o^2) = \left[\frac{\sum [w(F_o^2 - F_c^2)^2]}{\sum wF_o^4} \right]^{1/2}$$

filter (>495 nm) to the imaging spectrometer. The light sent to the spectrometer was directed toward the entrance slit, where it was reflected by a series of concave mirrors onto

TABLE 2
Atomic Coordinates and Equivalent Isotropic Displacement Parameters for (C₅H₁₄N₂)U₂O₄F₆ (AU1-3)

Atom	<i>x</i>	<i>y</i>	<i>z</i>	<i>U</i> _{eq} (Å ²) ^a
U(1)	0.0208(1)	0.3133(1)	0.2110(1)	0.022(1)
U(2)	0.4816(1)	0.1745(1)	0.2432(1)	0.023(1)
O(1)	0.1286(21)	0.3882(15)	0.3767(12)	0.044(3)
O(2)	-0.0850(21)	0.2394(15)	0.0452(13)	0.045(3)
O(3)	0.5764(21)	0.2504(16)	0.4068(13)	0.045(3)
O(4)	0.3924(21)	0.1039(14)	0.0762(12)	0.042(3)
F(1)	0.1056(13)	0.5469(10)	0.1743(10)	0.033(2)
F(2)	-0.2670(14)	0.3710(10)	0.2040(10)	0.036(2)
F(3)	-0.2270(14)	0.1229(10)	0.2589(10)	0.035(2)
F(4)	0.3454(14)	0.3644(10)	0.1932(11)	0.039(2)
F(5)	0.1472(14)	0.1169(11)	0.2484(11)	0.042(3)
F(6)	0.3978(15)	-0.0584(11)	0.2804(11)	0.042(3)
N(1)	0.5155(22)	0.7068(17)	0.2283(16)	0.038(4)
N(2)	0.9847(23)	0.7794(18)	0.2397(17)	0.046(4)
C(1)	0.6265(30)	0.6984(21)	0.3591(17)	0.044(5)
C(2)	0.8346(34)	0.8195(20)	0.4087(17)	0.045(5)
C(3)	0.9944(35)	0.7696(26)	0.3738(24)	0.064(7)
C(4)	0.8166(32)	0.7932(27)	0.1475(18)	0.052(5)
C(5)	0.6216(32)	0.6744(24)	0.1325(17)	0.051(6)

^a *U*_{eq} is defined as one-third of the trace of the orthogonalized *U*_{ij} tensor.

TABLE 3
Atomic Coordinates and Equivalent Isotropic Displacement Parameters for (C₅H₆N)UO₂F₃ (AU1-4)

Atom	<i>x</i>	<i>y</i>	<i>z</i>	<i>U</i> _{eq} (Å ²) ^a
U(1)	- $\frac{1}{2}$	$\frac{1}{4}$	-0.4568(1)	0.028(1)
O(1)	-0.2427(16)	$\frac{1}{4}$	-0.4570(5)	0.060(4)
F(1)	- $\frac{1}{2}$	$\frac{1}{4}$	-0.3281(7)	0.055(3)
F(2)	- $\frac{1}{2}$	-0.0628(10)	-0.4293(4)	0.044(2)
N(1)	0	$\frac{1}{4}$	-0.7675(11)	0.070(6)
C(1)	0	0.3452(32)	-0.6253(11)	0.071(5)
C(2)	0	0.4163(23)	-0.7321(13)	0.070(6)
C(3)	0	0.4812(56)	-0.6745(14)	0.054(8)

^a *U*_{eq} is defined as one-third of the trace of the orthogonalized *U*_{ij} tensor.

a prism and projected onto a CCD detector. Spectral image processing was performed on a PC using PARISS Software (Lightform Inc.). The exposure times used to achieve spectral resolution were 1000 ms for AU1-3 and 100 ms for both AU1-4 and AU1-5.

RESULTS AND DISCUSSION

Syntheses. The reactions of UO₃ with HF and homopiperazine, pyridine, or pyrazole in aqueous media at 180°C for 72 h result in the formation of (C₅H₁₄N₂)U₂O₄F₆ (AU1-3), (C₅H₆N)UO₂F₃ (AU1-4), and (C₃H₅N₂)UO₂F₃ (AU1-5), respectively. In all cases, the compounds can be isolated in high yield as large pale yellow to bright yellow crystals. The former compound crystallizes as needles and truncated rectangular bipyramids and the latter two exclusively as truncated rectangular bipyramids. The crystals are easily cleaved along the long axis of the crystal [100], in contrast to two- and three-dimensional uranium fluorides

TABLE 4
Atomic Coordinates and Equivalent Isotropic Displacement Parameters for (C₃H₅N₂)UO₂F₃ (AU1-5)

Atom	<i>x</i>	<i>y</i>	<i>z</i>	<i>U</i> _{eq} (Å ²) ^a
U(1)	0.4504(1)	$\frac{1}{2}$	-0.2979(1)	0.025(1)
O(1)	0.4508(5)	0.2354(22)	-0.2992(13)	0.044(3)
F(1)	0.3100(7)	$\frac{1}{2}$	-0.4124(17)	0.044(3)
F(2)	0.4239(7)	$\frac{1}{2}$	-0.6386(15)	0.036(3)
F(3)	0.5754(7)	$\frac{1}{2}$	0.0032(15)	0.036(3)
N(1)	0.2663(13)	$\frac{1}{2}$	0.0119(29)	0.047(5)
N(2)	0.2211(13)	$\frac{1}{2}$	-0.1872(28)	0.041(4)
C(1)	0.2116(15)	$\frac{1}{2}$	0.1050(32)	0.041(5)
C(2)	0.1303(13)	$\frac{1}{2}$	-0.0426(33)	0.042(5)
C(3)	0.1405(13)	$\frac{1}{2}$	-0.2218(34)	0.039(5)

^a *U*_{eq} is defined as one-third of the trace of the orthogonalized *U*_{ij} tensor.

and oxyfluorides, which are much harder, and do not cleave along planes easily.

Exploration of compositional space diagrams (20, 22, 24, 36–38) in these systems has provided the observation that reactions involving thermally robust aromatic amines, such as pyrazole and pyridine, result almost exclusively in U(VI)-containing products. Whereas the utilization of saturated amines such as homopiperazine, piperazine, and linear diamines often allows for the isolation of U(IV) compounds (18–20, 22, 23). Some of these compounds do not contain organic cations at all, but rather the amines have been completely degraded to ammonium cations (39). Reaction stoichiometries which lead to the isolation of **AU1-4**, when performed at 200°C do not result in the formation of new compounds or the observable decomposition of pyridine. This is in contrast to reactions involving homopiperazine where reactions of identical stoichiometry executed at 160, 180, or 200°C, resulted in different materials, some of which incorporated decomposition products of the amine (23). In nearly 2% of reactions involving pyridine or pyrazole, however, the formation of $\text{NH}_4\text{U}_3\text{F}_{13}$ in less than 1% yield was

observed (40), indicating that even aromatic amines can be decomposed under mild hydrothermal conditions, albeit to a much lesser extent than saturated amines. As these reactions occur in aqueous media, the participation of water in these redox reactions cannot be ruled out.

Structures: $(\text{C}_5\text{H}_{14}\text{N}_2)\text{U}_2\text{O}_4\text{F}_6$ (**AU1-3**), $(\text{C}_5\text{H}_6\text{N})\text{UO}_2\text{F}_3$ (**AU1-4**), and $(\text{C}_3\text{H}_5\text{N}_2)\text{UO}_2\text{F}_3$ (**AU1-5**). These structures are composed of linear one-dimensional chains formed from edge-sharing $[\text{UO}_2\text{F}_5]$ pentagonal bipyramids as shown in Fig. 1, and strongly hydrogen-bound protonated amines. Part of the structure of **AU1-5** with the pyrazolium cations included is shown in Fig. 2. The chains run down the *a*-axis in **AU1-3**, the *b*-axis in **AU1-4**, and the *c*-axis in **AU1-5**. The chains maintain linearity as they propagate through inversion or reflection of the pentagonal plane, which alternates the terminal fluoride vertex from one side to the other. **AU1-4** and **AU1-5** contain monocations for charge balance and therefore the repeating unit is $[\text{UO}_2\text{F}_3]^{1-}$. However, **AU1-3** contains diprotonated homopiperazine which doubles the repeating unit to $[\text{U}_2\text{O}_4\text{F}_6]^{2-}$. The fact that the

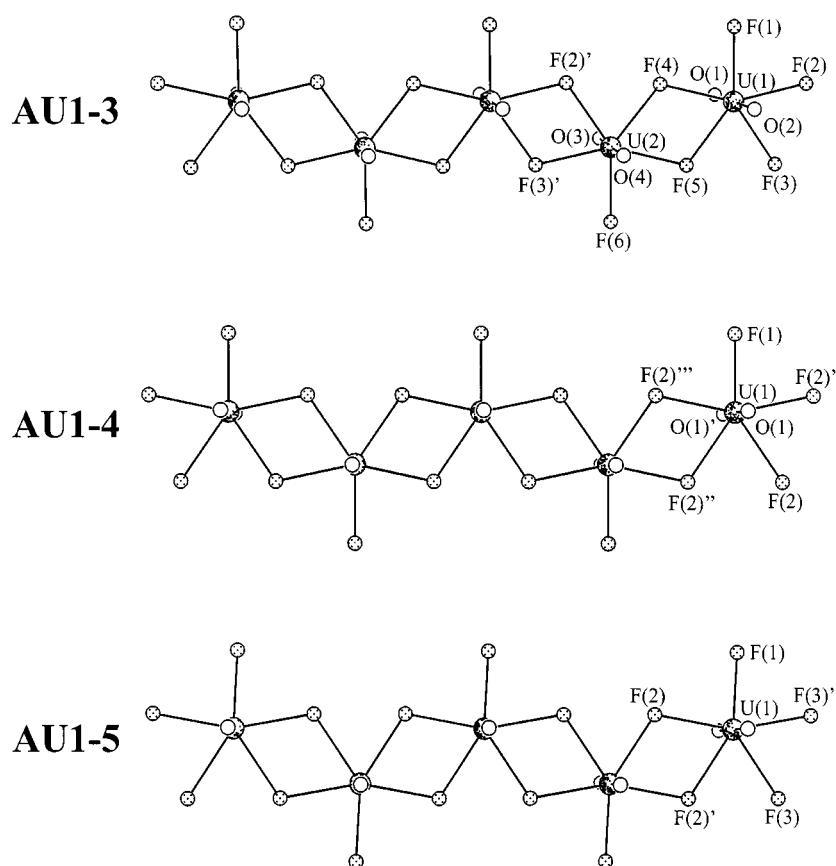


FIG. 1. (Top) $[\text{U}_2\text{O}_4\text{F}_6]^{2-}$ linear, one-dimensional chain that extends down the *a*-axis in $(\text{C}_5\text{H}_{14}\text{N}_2)\text{U}_2\text{O}_4\text{F}_6$ (**AU1-3**). (Middle) $[\text{UO}_2\text{F}_3]^{1-}$ linear, one-dimensional chain that extends down the *b*-axis in $(\text{C}_5\text{H}_6\text{N})\text{UO}_2\text{F}_3$ (**AU1-4**). (Bottom) $[\text{UO}_2\text{F}_3]^{1-}$ linear, one-dimensional chain that extends down the *c*-axis in $(\text{C}_3\text{H}_5\text{N}_2)\text{UO}_2\text{F}_3$ (**AU1-5**).

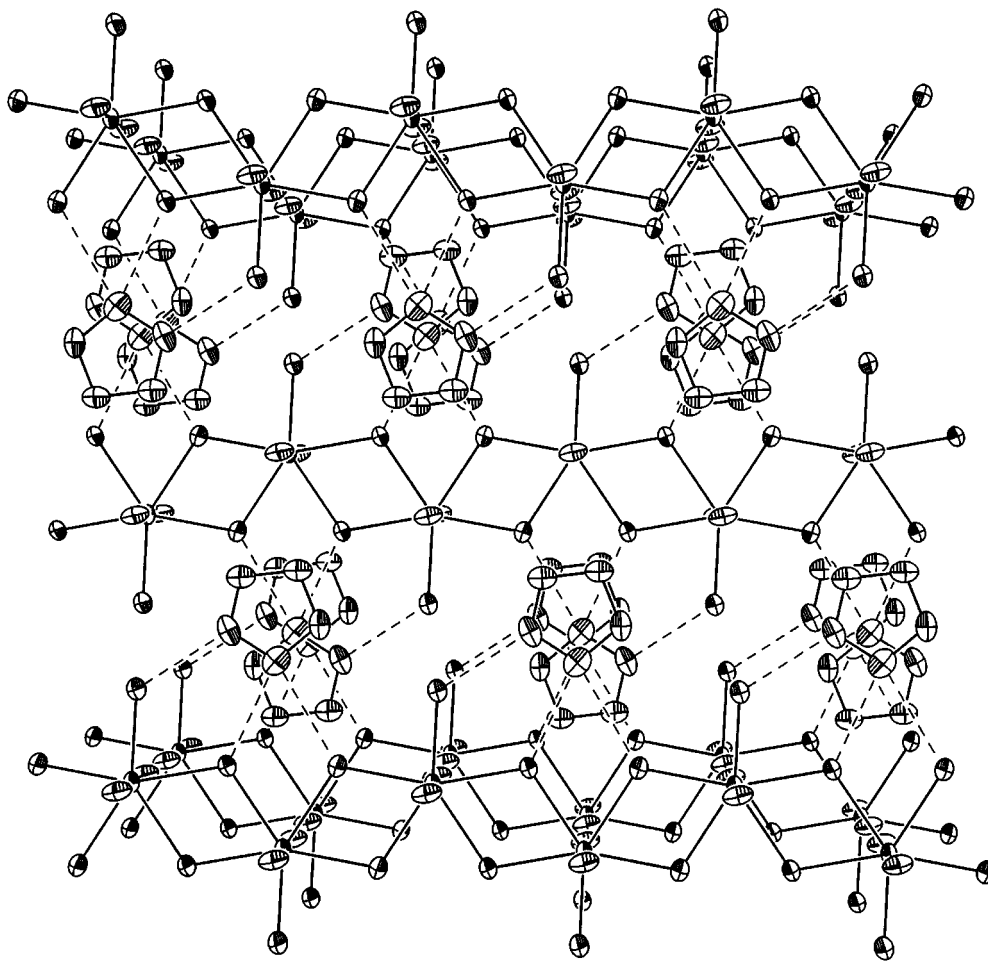


FIG. 2. A view along [010] of the linear, one-dimensional $[\text{UO}_2\text{F}_3]^{1-}$ chains in $(\text{C}_3\text{H}_5\text{N}_2)\text{UO}_2\text{F}_3$ (**AU1-5**) with hydrogen-bonded pyrazolium cations. 50% Displacement ellipsoids are shown.

same basic structures persist with three different cations of different size, shape, and charge argues against these structures being templated. Selected bond distances for **AU1-3**, **AU1-4**, and **AU1-5** are given in Table 5. The U–F bridging distances range from 2.296(9) to 2.355(9) Å, 2.311(7) to 2.372(7) Å, and 2.316(10) to 2.363(10) Å in **AU1-3**, **AU1-4**, and **AU1-5**, respectively. The U–F terminal distances are consistently shorter than bridging, and were found to be 2.216(9) and 2.213 Å in **AU1-3**, 2.200(11) Å in **AU1-4**, and 2.197(12) Å in **AU1-5**. As expected, the UO_2^{2+} moieties are approximately linear with bond angles of $179.5(6)^\circ$ and $177.7(6)^\circ$ for **AU1-3**, $179.8(5)^\circ$ for **AU1-4**, and $179.1(6)^\circ$ for **AU1-5**. The U=O bond distances are also within the expected ranges with distances from 1.748(11) to 1.771(13) Å being found.

Fluorescence spectroscopy. The differences in the fluorescence properties of **AU1-3**, **AU1-4**, and **AU1-5** were first

noted using a hand-held UV lamp. The emission of green light from **AU1-4** and **AU1-5** is easily observed when the samples are irradiated with 365-nm UV light. Emission from **AU1-3**, however, is considerably weaker and barely observable with the naked eye. The fluorescence of compounds containing uranyl units is well known both in the solid state and in solution and is easily identified from the vibronic fine-structure characteristic of the UO_2^{2+} moiety (41, 42). In order to probe this in a semiquantitative fashion, absorption and emission spectra for **AU1-3**, **AU1-4**, and **AU1-5** were collected from single crystals of approximately the same size using optical microscopy. **AU1-3**, **AU1-4**, and **AU1-5** show typical emission features for uranyl compounds with considerable fine structure present. The emission spectra of these three compounds are shown in Fig. 3. These spectra are also consistent with those obtained for other uranyl-containing materials and indicate that **AU1-3** does indeed fluoresce weaker than **AU1-4** or **AU1-5**, as

TABLE 5
**Selected Bond Distances (Å) for (C₅H₁₄N₂)U₂O₄F₆ (AU1-3),
 (C₅H₆N)UO₂F₃ (AU1-4), and (C₃H₅N₂)UO₂F₃ (AU1-5)**

(C ₅ H ₁₄ N ₂)U ₂ O ₄ F ₆ (AU1-3)			
U(1)–O(1)	1.771(13)	U(2)–O(4)	1.778(13)
U(1)–O(2)	1.769(14)	U(2)–F(2)′	2.355(9)
U(1)–F(1)	2.216(9)	U(2)–F(3)′	2.296(9)
U(1)–F(2)	2.318(9)	U(2)–F(4)	2.344(9)
U(1)–F(3)	2.354(9)	U(2)–F(5)	2.360(9)
U(1)–F(4)	2.347(9)	U(2)–F(6)	2.213(9)
U(1)–F(5)	2.338(9)	U(1)–U(2)	3.9208(12)
U(2)–O(3)	1.752(14)	U(2)–U(1)′	3.8953(13)
(C ₅ H ₆ N)UO ₂ F ₃ (AU1-4)			
U(1)–O(1)	1.748(11)	U(1)–F(2)′	2.311(7)
U(1)–O(1)	1.748(11)	U(1)–F(2)′	2.372(7)
U(1)–F(1)	2.200(11)	U(1)–F(2)′	2.372(7)
U(1)–F(2)	2.311(7)	U(1)–U(1)	3.9062(10)
(C ₃ H ₅ N ₂)UO ₂ F ₃ (AU1-5)			
U(1)–O(1)	1.77(2)	U(1)–F(3)	2.363(10)
U(1)–O(1)′	1.77(2)	U(1)–F(3)′	2.334(10)
U(1)–F(1)	2.197(12)	U(1)–U(1)	3.947(2)
U(1)–F(2)	2.316(10)	U(1)–U(1)′	3.904(2)
U(1)–F(2)′	2.357(10)		

a 10-fold exposure time was needed to obtain spectra of similar intensities (30, 41, 42). The striking difference is that emission from **AU1-3** shows much broader features than the other two compounds.

There are several explanations that account for the spectral differences between **AU1-3** and **AU1-4** and **AU1-5**. One possibility is that partial quenching of the excited state in **AU1-3** may be occurring via proton or electron transfer. Electron-transfer can be ruled out, as a suitable chromophore is not present in **AU1-3**. However, proton transfer is not so easily dismissed owing to the substantial hydrogen-bonding in all of these compounds. Grohol and Clearfield also recently reported variances in the luminescent properties of two closely related uranyl phosphonates, [UO₂(HO₃PC₆H₅)₂(H₂O)]₂·8H₂O and UO₂(HO₃PC₆H₅)₂(H₂O)·2H₂O, whose structural differences are based largely on conformational differences in the phosphonates (30).

Instead of viewing this disparity as quenching of **AU1-3**, it could be viewed as actually arising from enhancement of the fluorescence in **AU1-4** and **AU1-5** versus **AU1-3**. This reasoning is particularly strong since protonated aromatic amines (i.e., pyridinium) fluoresce, and the observed emission is derived solely from the uranyl group, not from the pyridinium or pyrazolium cations. Energy transfer from pyridinium and pyrazolium to the uranyl moieties could therefore enhance the observed fluorescence of **AU1-4** and **AU1-5** relative to **AU1-3**. The broadened features in **AU1-3** may be due to its reduced symmetry versus **AU1-4** and

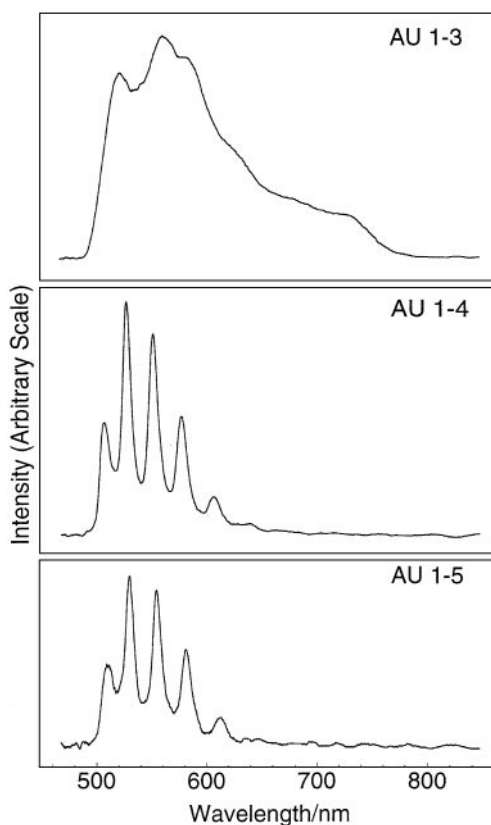


FIG. 3. Emission spectra of (C₅H₁₄N₂)U₂O₄F₆ (**AU1-3**) (a), (C₅H₆N)UO₂F₃ (**AU1-4**) (b), and (C₃H₅N₂)UO₂F₃ (**AU1-5**) (c).

AU1-5, as there are two crystallographically unique uranyl groups, which might lead to small shifts in absorption and emission and give rise to mechanisms for non-radiative decay.

CONCLUSIONS

The hydrothermal synthesis of low-dimensional and open-framework uranium-containing compounds continues to yield materials with unprecedented structures and potentially useful physicochemical properties. Compositional space diagrams are extremely useful in these explorations, particularly when searching for appropriate reaction stoichiometries for producing pure compounds (20, 22, 24, 36–38). The use of this methodology has allowed for the isolation of many new materials that will be the subject of future reports.

Auxiliary material. Tables of anisotropic displacement parameters and structure factors for **AU1-3**, **AU1-4**, and **AU1-5** (24 pages) are available from the corresponding author upon request.

ACKNOWLEDGMENTS

This work was supported by NASA (Alabama Space Grant Consortium), NASA-EPSCoR, and Auburn University. R. Blumenthal, V. Cammarata, and M. E. Squillacote are also acknowledged for helpful discussions of fluorescence spectroscopy.

REFERENCES

1. A. Rabenau, *Angew. Chem. Int. Ed. Engl.* **24**, 1026 (1985).
2. J. W. Kolis and M. B. Korzenski, in "Chemical Synthesis Using Supercritical Fluids" (P. G. Jessop and W. Leitner Eds.), Chap. 4. Wiley-VCH, New York, 1999.
3. A. K. Cheetham, G. Férey, and T. Loiseau, *Angew. Chem. Int. Ed. Engl.* **38**, 3268 (1999). [And references therein]
4. D. R. Corbin, J. F. Whitney, W. C. Fultz, G. D. Stucky, M. M. Eddy, and A. K. Cheetham, *Inorg. Chem.* **25**, 2279 (1986).
5. D. Riou, F. Taulelle, and G. Férey, *Inorg. Chem.* **35**, 6392 (1996).
6. P. Feng, X. Bu, and G. D. Stucky, *Nature* **388**, 735 (1997).
7. P. Feng, X. Bu, and G. D. Stucky, *Chem. Mater.* **11**, 3025 (1999).
8. H. Li, M. Eddaoudi, and O. M. Yaghi, *Angew. Chem. Int. Ed. Engl.* **38**, 653 (1999).
9. A. Choudhury, S. Natarajan, and C. N. R. Rao, *Chem. Mater.* **11**, 2316 (1999).
10. M. Riou-Cavellec, M. Sanselme, and G. Férey, *J. Mater. Chem.* **10**, 745 (2000).
11. S. T. Wilson, B. M. Lok, C. A. Messina, T. R. Cannan, and E. M. Flanigen, *J. Am. Chem. Soc.* **104**, 1146 (1982).
12. E. M. Flanigen, R. L. Patton, and S. T. Wilson, *Stud. Surf. Sci. Catal.* **37**, 13 (1988).
13. T. E. Gier and G. D. Stucky, *Nature* **349**, 508 (1991).
14. R. Xu, J. Chen, and C. Feng, *Stud. Surf. Sci. Catal.* **60**, 63 (1991).
15. A. Clearfield, *Chem. Rev.* **88**, 125 (1988).
16. A. M. Fogg, J. S. Dunn, S.-G. Shyu, D. R. Cary, and D. O'Hare, *Chem. Mater.* **10**, 351 (1998).
17. M. E. Davis and R. F. Lobo, *Chem. Mater.* **4**, 756 (1992).
18. R. J. Francis, P. S. Halasyamani, and D. O'Hare, *Chem. Mater.* **10**, 3131 (1998).
19. R. J. Francis, P. S. Halasyamani, and D. O'Hare, *Angew. Chem. Int. Ed. Engl.* **37**, 2214 (1998).
20. R. J. Francis, P. S. Halasyamani, J. S. Bee, and D. O'Hare, *J. Am. Chem. Soc.* **121**, 1609 (1999).
21. P. S. Halasyamani, S. M. Walker, and D. O'Hare, *J. Am. Chem. Soc.* **121**, 7415 (1999).
22. S. M. Walker, P. S. Halasyamani, S. Allen, and D. O'Hare, *J. Am. Chem. Soc.* **121**, 10,513 (1999).
23. P. M. Almond, L. Deakin, M. J. Porter, A. Mar, and T. E. Albrecht-Schmitt, *Chem. Mater.*, in press (2000).
24. P. S. Halasyamani, R. J. Francis, S. M. Walker, and D. O'Hare, *Inorg. Chem.* **38**, 271 (1999).
25. R. J. Francis, M. J. Drewitt, P. S. Halasyamani, C. Ranganathachar, D. O'Hare, W. Clegg, and S. J. Teat, *Chem. Commun.* **2**, 279 (1998).
26. D. M. Poojary, D. Grohol, and A. Clearfield, *J. Phys. Chem. Solids* **56**, 1383 (1995).
27. D. M. Poojary, D. Grohol, and A. Clearfield, *Angew. Chem. Int. Ed. Engl.* **34**, 1508 (1995).
28. D. Grohol, M. A. Subramanian, D. M. Poojary, and A. Clearfield, *Inorg. Chem.* **35**, 5264 (1996).
29. D. M. Poojary, A. Cabeza, M. A. G. Aranda, S. Brugue, and A. Clearfield, *Inorg. Chem.* **35**, 1468 (1996).
30. D. Grohol and A. Clearfield, *J. Am. Chem. Soc.* **119**, 4662 (1997).
31. J. H. Burns, in "The Chemistry of the Actinide Elements" (J. J. Katz, G. T. Seaborg, and J. R. Morss, Eds.), Chap. 20. Chapman & Hall, London, 1986.
32. P. H. Brusset, N. Q. Dao, and S. Chourou, *Acta Crystallogr. B* **30**, 768 (1974).
33. Y. N. Mikhailov, A. A. Udovenko, V. G. Kuznetsov, L. A. Butman, and L. A. Kokh, *J. Struct. Chem.* **13**, 879 (1972).
34. G. M. Sheldrick, SHELXTL PC, Version 5.0, An Integrated System for Solving, Refining, and Displaying Crystal Structures from Diffraction Data. Siemens Analytical X-Ray Instruments, Inc., Madison, WI, 1994.
35. W. H. Zachariasen, *Acta Crystallogr. B* **1**, 277 (1948).
36. P. S. Halasyamani, M. J. Willis, P. M. Lundquist, C. L. Stern, G. K. Wong, and K. R. Poeppelmeier, *Inorg. Chem.* **35**, 1367 (1996).
37. W. T. A. Harrison, L. L. Dussack, and A. J. Jacobson, *J. Solid State Chem.* **125**, 234 (1996).
38. A. J. Norquist, K. R. Heier, C. L. Stern, and K. R. Poeppelmeier, *Inorg. Chem.* **37**, 6495 (1998).
39. P. M. Almond, L. Deakin, M. J. Porter, A. Mar, and T. E. Albrecht-Schmitt, submitted for publication (2000).
40. P. H. Abazli, A. Cousson, A. Tabuteau, and M. Pagès, *Acta Crystallogr. B* **36**, 2765 (1980).
41. W. T. Carnall and H. M. Crosswhite, in "The Chemistry of the Actinide Elements" (J. J. Katz, G. T. Seaborg, and J. R. Morss, Eds.), Chap. 16. Chapman & Hall, London, 1986.
42. R. G. Denning, J. O. W. Norris, I. G. Short, T. R. Snellgrove, and D. R. Woodward, "Lanthanide and Actinide Chemistry and Spectroscopy" (ACS Symp. Ser. No. 131) (N. M. Edelstein, Ed.), Chap. 15. Am. Chem. Soc. Washington, DC, 1980.